

Effects of root properties and branching characteristics on soil reinforcement in the Jinyun Mountain, China

Shuangshuang Song¹, Yunqi Wang^{2,*}, Baoping Sun¹ and Yunpeng Li³

¹School of Soil and Water Conservation, and

²Jinyun Forest Ecosystem Research Station, Beijing Forestry University, Beijing 100083, People's Republic of China

³China Academy of Transportation Sciences, Beijing 100029, People's Republic of China

Plant roots can substantially improve slope stability and prevent soil slippage. Many researchers have quantified effects of root properties on soil reinforcement. However, the mechanism of root architecture on shear strength increments needed to be studied and analysed. This paper presents a man-made direct shear test to compare the effects of six tree species roots on soil reinforcement. Thus, root tensile strength, diameter, root area ratio (RAR), inclination and distribution were measured to study the differences between root architecture. Meanwhile, stress propagation simulations were conducted to analyse the mechanisms of root architecture on soil reinforcement. Results showed that shear strength increment value corresponded to *P. massoniana* (42.4 kPa), followed by *C. camphora* (37.6 kPa), *N. aurata* (36.0 kPa), *L. kwangtungensis* (28.8 kPa), *G. acuminata* (27.4 kPa) and *S. laurina* (23.0 kPa). Root architecture that contained taproots (VH-type) and widely distributed roots (H-type) showed larger shear strength increments than that contained oblique roots (R-type) when the initial friction between soil and root was ignored. When there are thick, widely distributed roots in the root system, the resistance of root architecture on shear failure would become larger. Root diameter class and RAR cannot be used to reflect the effects of root architecture on soil shear strength increment. While estimating the different tree species roots on soil reinforcement in field, initial friction between soil and root should be considered as important as root architecture.

Keywords: Root architecture, root properties, shear test, shear strength increment, stress propagation simulation.

THE use of plants to prevent soil erosion and shallow landslides has become a recognized ecological engineering method throughout the world. Enhancement of slope stability by plants is mainly due to the roots¹. Roots can substantially improve slope stability and prevent soil slippage in two ways – hydrological^{2–4} and mechanical^{5,6}.

However, mechanical methods contribute much more in preventing shallow landslides than hydrological factors when there are no extreme rainfall events^{1,7}. Mechanical factors of root reinforcements on slope stability can be classified as: (1) soil–root interface properties⁸; (2) root properties such as root tensile strength, density, diameter, root area ratio (RAR) and root length density, etc.⁹; (3) branching characteristics such as root distribution, inclination and architecture¹⁰. Many studies have been made both analytically and experimentally^{11–13}. Wu *et al.*¹¹ proposed a simple root reinforcement model based on the force equilibrium principle, to evaluate the shear strength increment provided by roots. Over the years, more models and methods have been developed such as fibre bundle models¹⁴, finite element analysis¹⁵, man-made direct shear box tests¹³ and numerical simulations¹⁶.

Soil–root interface properties are deemed to be the most important factor on soil shear strength increments, followed by branching characteristics and root properties. In the case of mechanical mode of root reinforcements, pull-out tests¹⁷ and shear tests¹³ are the most common methods due to their simple design principles than any other methods. Fan and Chen⁹ had applied *in situ* shear box to study the effect of root architecture on soil shear strength increment. They discussed in detail the young trees' root architecture on soil strength increments using Yen's classification¹⁸. They suggested that root architecture had a large impact on soil strength increments, and that variation of root architecture was decided by spatial heterogeneity and environmental differences. Prasad *et al.*¹⁹ also studied the effect of roots on soil shear strength with the same method. They compared the effects of roots and live poles on soil shear strength increments and found that a greater strength was observed in rooted soil samples due to influence of root spatial distribution. Although their results showed that roots had a positive role in soil reinforcement, for certain study areas, more detailed effects of root architecture and root spatial distribution characteristics on shear strength increments need to be studied and analysed.

This paper aims to investigate root properties and branching characteristics of root architecture and root

*For correspondence. (e-mail: wangyunqibj@163.com)

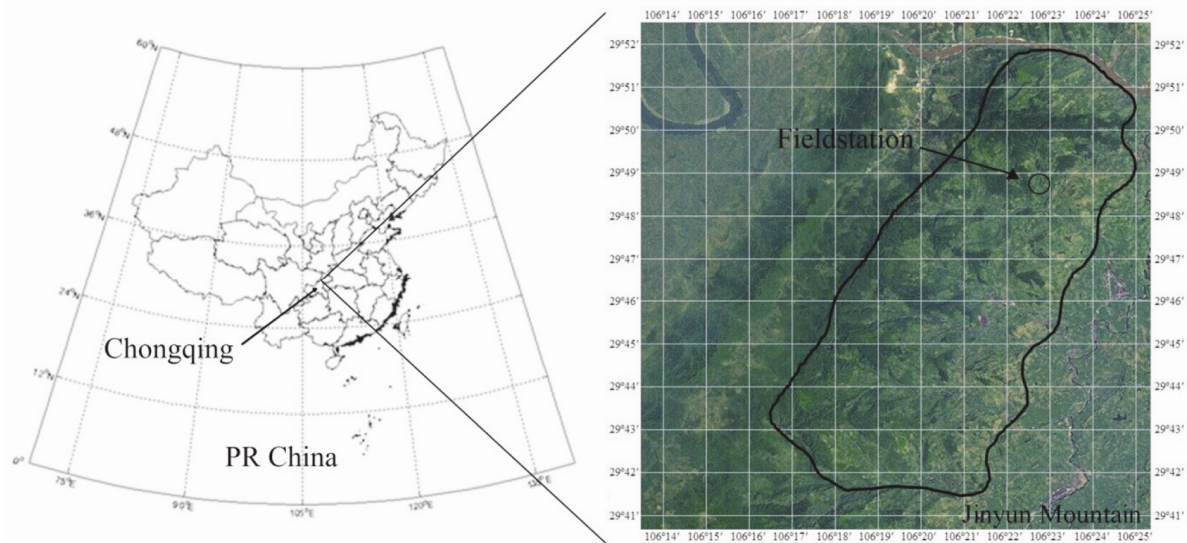


Figure 1. Location of Jinyun Mountain in Chongqing, China.

spatial distribution on soil shear strength increments. Man-made direct shear tests for six tree species roots are conducted. In addition, stress propagation simulations were used to analyse mechanisms of root architecture on the strength increments. Root tensile strength, diameter, RAR, inclination and distribution were measured and compared combining with the results of stress propagation simulation. Our results can provide a reference for further studies on mechanical modes of root reinforcement on soil shear strength and help in proper species selections for ecological engineering construction in the southwest of China.

Materials and methods

Study area

The study area is located on Jinyun Mountain in Beibei, Chongqing, China (Figure 1). Geographic coordinates are 106°22'E, 29°45'N. The Jinyun Mountain covers an area of 76 km². It has a typical subtropical monsoon climate with an annual average temperature of 13.6°C. The highest elevation is 951 m. Due to high annual average rainfall (1783.8 mm), it has a large area of evergreen broad-leaved forest. Soil in Jinyun Mountain area is derived from Triassic Xujiahe Formation sandstone and shale. Soil types are orthic acrisols and a small amount of aric anthrosols²⁰. Tree samples were taken from the south of Jinyun Mountain, on an average slope of 5°.

Tree species and root architecture

Sampling tree species were: *Pinus massoniana* Lamb, *Cinnamomum camphora* (L.) Presl, *Lindera kwangtungensis* (Liou) Allen, *Gordonia acuminata*, *Neolitsea*

aurata var. *glauca* and *Symplocos laurina* (Retz) Wall. The first three are tall tree species, and the rest are small tree species. They are all dominant tree species on Jinyun Mountain (Figure 2). *P. massoniana* and *G. acuminata* are taproot types with thick and long taproot and fine and short lateral roots. *C. camphora* and *N. aurata* have shallow root systems with few vertical roots which extend horizontally and widely. *L. kwangtungensis* and *S. laurina* have the most lateral roots. Roots have a wide lateral extent. Using the Yen's classification¹⁸, root architectures were divided into three types: VH-type (*P. massoniana* and *G. acuminata*), H-type (*C. camphora* and *N. aurata*) and R-type (*L. kwangtungensis* and *S. laurina*). Root architecture characteristics of six tree species are shown in Table 1 and Figure 2.

During sample collection, trunk part of the plants was truncated and removed. Isolated juvenile plants, with no neighbours within a 0.5 m radius, were selected to limit plant–plant interactions, which could dramatically affect root system development, and to make sampling easier. In addition, as young trees were sampled, plant age could not be determined accurately, so, both basal diameter threshold value of 20 mm and the same growing conditions for all tree species were used. Based on field observation, growth depth of each root was not more than 0.5 m. Thus, we dug to a depth of 0.6 m to make sure a complete root system could be obtained. Each plant was carefully excavated by hand to keep the root system intact. After wiping off the soil on the roots, samples were packed in black plastic bags and taken to the laboratory for subsequent experiments.

Soil

Soil was collected from the same location where trees species were dug up. To ensure effective results for the

Table 1. Classification of root architecture for six tree species used in this study

Species	Description of root architecture	Classification based on Yen ¹⁸
<i>S. laurina</i>	Most of the main roots grow obliquely. Lateral roots are observed in some of the samples	R-type
<i>L. kwangtungensis</i>	Roots have a wide lateral extent	
<i>P. massoniana</i> <i>G. acuminata</i>	Plants with strong taproots. Lateral roots extend widely and in low orientation with respect to the horizontal plane	VH-type
<i>N. aurata</i> <i>C. camphora</i>	Most of the roots extend horizontally and widely	H-type

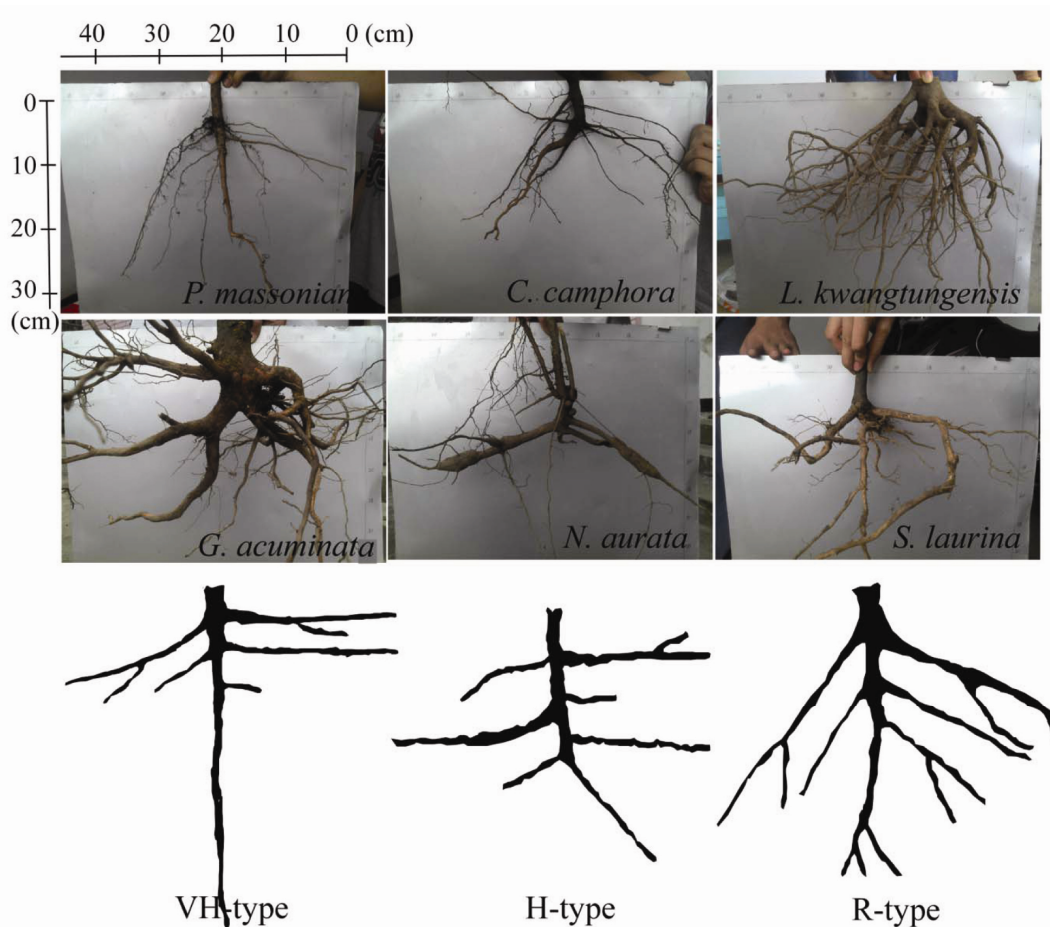


Figure 2. Pictures of root architecture for six tree species.

shear process, soil samples in shear box were required to be of the same physical and chemical properties. Thus, soil in the depth of 20–30 cm below the earth’s surface was collected and used in this study. After removing biological impurities from the soil by hand, 2 m³ volume of soil samples were taken to the laboratory. In order to maintain same soil moisture content in each shear test, a Soil Moisture Analyzer (SC900, SPECTRUMTDR, USA) was used to measure the moisture content of soil samples. In the first test, the moisture content of the soil sample was 21.7%. In the subsequent tests, soil moisture content remained around 20%. Since the moisture content

dropped after each test, a sprinkling-can was used to add water into soil samples to ensure a homogenous test process. In the whole experiment process, soil moisture content changed at a range of 19.2–23.4%.

Characteristics of root structure

Root diameter class and RAR: Based on the buried depth of the roots in the test (force distribution of shearing field was 100 mm deep below earth’s surface), the root diameter within 50–150 mm of depth was classified into 6

groups: 0–2 mm, 2–4 mm, 4–6 mm, 6–8 mm, 8–10 mm and 10+ mm. For each root, we measured root diameter at its base, tortuous and straight root lengths. Then the average of all diameters was used to represent one root diameter. RAR can be calculated as follows

$$\text{RAR} = \frac{\sum_{i=1}^N \frac{\pi n_i d_i^2}{4}}{A} (N = 5), \quad (1)$$

where n_i represents the number of roots in each diameter level, d_i represents median diameter of each diameter level (mm), A represents the area of shear box, N represents the number of diameter class classification.

Root tensile strength measurement: Root tensile strength (T_R) tests were performed with S9M Universal Mechanical Testing Machine (Shanghai, China). Damaged roots were discarded for the tests. Root samples of approximately 60 mm in length were selected for testing. Before the test, we tied the two root ends with tapes to increase friction and then moved at a constant speed of 0.02 m/min to apply a tensile force to the root. When the root ruptured, the diameter of the breaking point was measured using a caliper. Due to the presence of root bark, the success rate of the test result was just 40–50%. For each plant, the number of successful trials need to be more than 40. According to Operstein and Frydman²¹, T_R decreased with increasing root diameter following a simple power law equation of

$$T_R = aD^{-b}, \quad (2)$$

where T_R represents root tensile strength (MPa); D represents root diameter (mm); a and b are constants.

Shear tests of root

Shear tests are conducted with man-made direct shear machine which consists of support system (shelf), force application system (hand shank and a feed screw), measurement system (tautness meter and dividing rule) and sample container (shear box) (Figure 3). The length, width and height of the shear box are 300 × 300 × 200 mm. The box's body material is 10 mm thick PVC board, which is internally polished to reduce frictions between soil and inner walls of the box. In order to get stable experimental environment, shear box was fixed on a cement floor in the lab. There were boards on both sides of the box to prevent oblique sliding. Before tests, shear box was aligned and the tension meter was adjusted to 0. We added soil samples into the shear box up to a thickness of 50 mm. A lid was used to compact surface soil so that soil compaction was approximate with natural conditions. Soil samples are considered compacted when the thickness reaches 40 mm. We then placed the roots inside

the box (before samples were placed in the box, roots were photographed towards the shear direction), and soil samples were added as before. Altogether, the soil sample was added five times into the shear box in one test so that the roots are fully in contact with the soil. Later, we rotated the handle by hand with a homogeneous velocity of 5 S/ring, and then shear test was performed at a constant displacement rate of 0.024 m/min. As the effects of root reinforcements were different, we assumed that when shear displacement reached at 26 mm, it then stopped. After each shear test, soil samples and roots were removed from the shear box. Soil samples were loosened by hand and soil moisture content was adjusted. Soil samples were reloaded into the shear box with new roots. Finally, data of tautness meter and diving rule were recorded and analysed. There are three replicates for each tree species. Shear tests of soil with no roots were also conducted in this study. Eighteen soil samples with roots and three soil samples without roots were tested in this experiment.

Soil reinforcement model

To evaluate the potential increase in soil shear strength due to roots, two methods, ΔS_w and ΔS_i were applied in our study. ΔS_i represents root architecture strength which is calculated by shear tests. Due to different experimental measurements, root and soil samples were not carried out together in field. The original friction between roots and soil (friction under natural conditions) was broken and later root and soil samples were placed in the shear box. So ΔS_i is only affected by root properties and root architecture. ΔS_w is referenced using Wu's model¹¹

$$\Delta S_w = 1.2t_R, \quad (3)$$

where t_R represents root tensile strength per unit area of soil, kPa. In order to account for root diameters variability, eq. (3) has to be written as follows, taking into account T_R and RAR for different diameter classes

$$t_R = \sum_{i=1}^N \frac{T_{Ri} A_i}{A} (N = 5). \quad (4)$$

Stress propagation simulation

To study the stress propagation of rooted soil samples under shear forces, a 3D model was established using MIDAS (MIDAS IT, China). The model consists of soil and a single root. The length, width and height of the simulation model are 300 × 10 × 200 mm. Interface of soil and root is strict contact (the elastic–plastic properties of interface are consistent). The simulation model boundaries with their normal in x -direction are fixed in

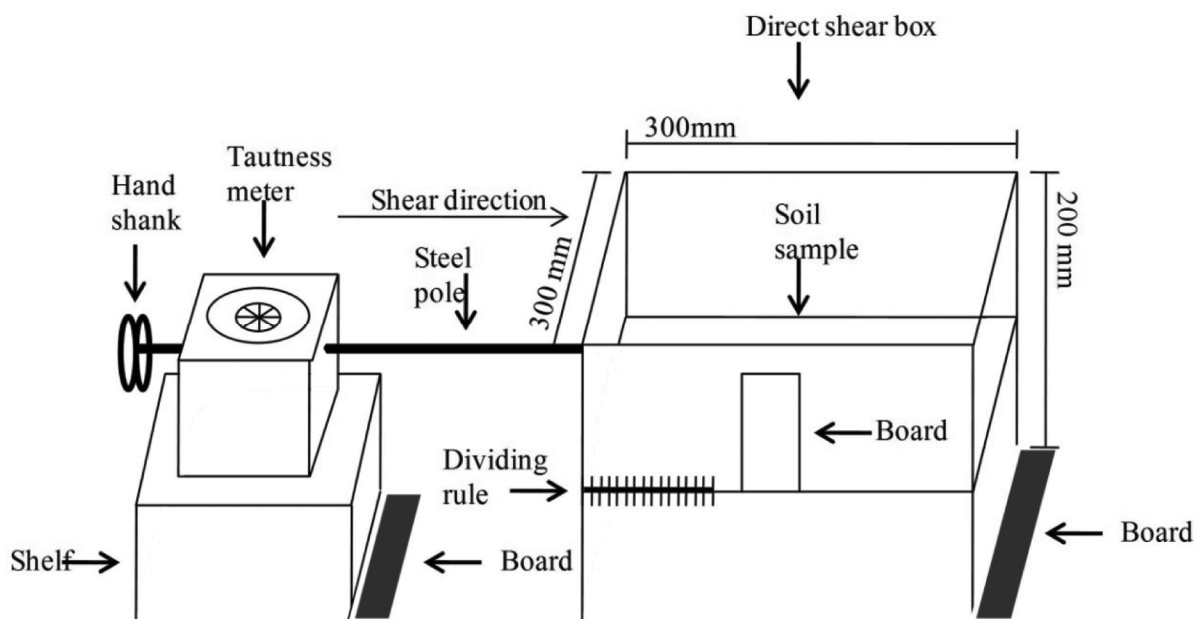


Figure 3. Schematic diagram of the man-made direct shear machine.

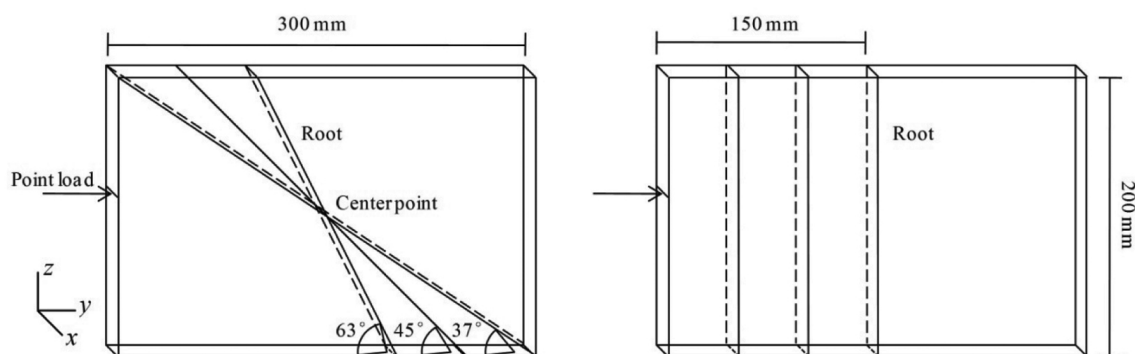


Figure 4. Schematic diagram of stress propagation simulation.

z-direction and free in x- and y-directions. The simulation model boundaries with their normal in y-direction are fixed in x-direction and free in y- and z-directions. The bottom boundary of the finite element mesh is fixed against displacement in x-, y-, and z-directions. Unit weight of the soil was 13.5 kN/m³. Soil modulus of elasticity was 6 MPa and a Poisson's ratio of 0.3, were referenced in Fan and Lai's work²². Simulation root length was 200 mm to 360.6 mm. Elastic modulus of fine and thick root was 200 MPa and 400 MPa respectively²¹. A point load was used to simulate collapsing force, which was 100 N in horizontal direction from the centre of the simulation model. Stress propagation simulation of roots is shown in Figure 4. There were two situations that existed in stress propagation simulation. In the first situation, root was placed inclined in soil samples, at an angle in horizontal direction. The inclination of the roots was 63°, 45° and 37° respectively. In the second situation, dif-

ferent distances between root and load point were simulated to study changes of stress propagation in soil samples. Also, we assumed three distances (50 mm, 100 mm and 150 mm) as shown in Figure 4.

Results

Comparison of shear strength between tree species

Relationship between shear strength and shear displacement of tree species is shown in Figure 5. *P. massoniana*, *C. camphora* and *L. kwangtungensis* showed shear failure at 12 mm displacement, whereas *G. acuminata*, *N. aurata* and *S. laurina* showed at 16 mm displacement. Before shear failure, soil shear strength increased rapidly with displacement and after shear failure, the soil shear strength tended to be stable. Peak shear strength values

Table 2. Characteristics of six tree species. RAR was measured at a depth of 100 mm at the location of shear plane

Species	Root diameter class (mm)						RAR (%)
	0–2	2–4	4–6	6–8	8–10	10 and above	
<i>L. kwangtungensis</i>	25.0	11.7	7.0	4.0	1.7	1.0	0.05801
<i>S. laurina</i>	12.3	6.3	4.3	1.0	0.7	1.0	0.03000
<i>P. massoniana</i>	10.0	2.0	0.3	0.3	0.3	0	0.00585
<i>G. acuminata</i>	18.7	4.3	2.3	0.7	0.7	0.7	0.02166
<i>N. aurata</i>	11.7	3.7	2.7	0.7	0.3	0	0.01343
<i>C. camphora</i>	15.7	2.7	0.3	0.7	0.7	0.7	0.01637

Table 3. Regression equations between root tensile strength (T_R , MPa) and root diameter D (mm)

Species	Regression equation	R^2
<i>L. kwangtungensis</i>	$T_R = 76.15D^{-1.06}$	0.81
<i>S. laurina</i>	$T_R = 83.79D^{-0.63}$	0.78
<i>P. massoniana</i>	$T_R = 44.01D^{-0.60}$	0.76
<i>G. acuminata</i>	$T_R = 77.71D^{-0.96}$	0.92
<i>N. aurata</i>	$T_R = 97.80D^{-0.82}$	0.85
<i>C. camphora</i>	$T_R = 69.51D^{-0.48}$	0.71

were found for the different tree species. The highest peak value corresponded to *P. massoniana* (66.7 kPa), followed by *C. camphora* (64.4 kPa), *G. acuminata* (61.1 kPa), *N. aurata* (58.9 kPa), *S. laurina* (53.9 kPa) and *L. kwangtungensis* (51.7 kPa). The same relationship also existed for the average peak shear strength for each tree species, like *P. massoniana* (61.7 kPa), *C. camphora* (56.9 kPa), *G. acuminata* (56.1 kPa), *N. aurata* (55.3 kPa), *L. kwangtungensis* (48.1 kPa) and *S. laurina* (42.3 kPa). VH-type roots showed best resistance for shear failure, but expressed shorter displacement when shear failure occurred. Despite the weaker shear strength of H-type, it had endured longer displacement when shear failure occurred. R-type showed the worst performance of resistance for shear failure. For the same root architecture, differences between shear strength were 1.6 kPa and 5.6 kPa whereas for different root architecture, differences between shear strength were 0.8 kPa and 9.4 kPa.

Characteristics of root architecture

The characteristics of tree species are shown in Table 2. The smallest diameter roots (0–2 mm) existed in *L. kwangtungensis*. Medium diameter roots were mostly found in R-type which mainly consist of oblique roots. Roots with large diameters were often found in widely distributed root architecture (H-type). R-type had the largest value of RAR, which was 0.058101% (*L. kwangtungensis*), followed by VH- and H-type. *P. massoniana* (VH-type) had the minimum value of RAR which was 0.00585%.

Root tensile strength and root reinforcement

Table 3 shows results of the tensile strength tests for roots of six tree species. Root tensile strength differed between tree species. Values of a ranged from 44.01 to 97.80, while b ranged from -0.48 to -1.06 . Only *L. kwangtungensis* obtained b lesser than -1 . Tall tree species had greater value of a than small tree species, which could reach up to 1.56–39.78. There was no rule on tensile strengths of different root architectures.

Results of ΔS_w and ΔS_t are listed in Table 4. *S. laurina* had a maximum value of ΔS_w at 473.7 kPa. The minimum value of ΔS_w was seen in *P. massoniana* (61.3 kPa). ΔS_w differed between root architecture; R-type showed the largest value of ΔS_w , followed by H-type and VH-type. Shear strength of soil without roots was 19.3 kPa during shear tests. However, ΔS_t had showed an opposite relationship with ΔS_w (*S. laurina* had the minimum ΔS_t of 23.0 kPa and *P. massoniana* had the maximum ΔS_t of 42.4 kPa). In order to compare ΔS_w and ΔS_t , we introduced a concept called ‘efficiency of root architecture’ which was ΔS_t divided by ΔS_w . It can be used to represent the contributions of root architecture and root properties on shear strength increment. Efficiency of root architecture ranged from 4.9% to 69.2%. For the same root architecture, the average of efficiency of VH-type was 43.5%, followed by H-type (15.0%) and R-type (5.7%).

Shear strength increment compared with root architecture characteristics showed no relationship with RAR (Figure 6). When the value of RAR was maximum in *L. kwangtungensis* (0.058101%), the corresponding shear strength increment in *L. kwangtungensis* reached at only 28.8 kPa which was the second smallest value of shear strength increment. Although other studies reported that RAR led to an increase of shear strength increment²³, we observed no correlation between shear strength increment and RAR.

Characteristics of root spatial distribution

Spatial distribution of different root architecture characteristics (root inclination and distribution) is shown in Figure 7. Root branching characteristics are measured

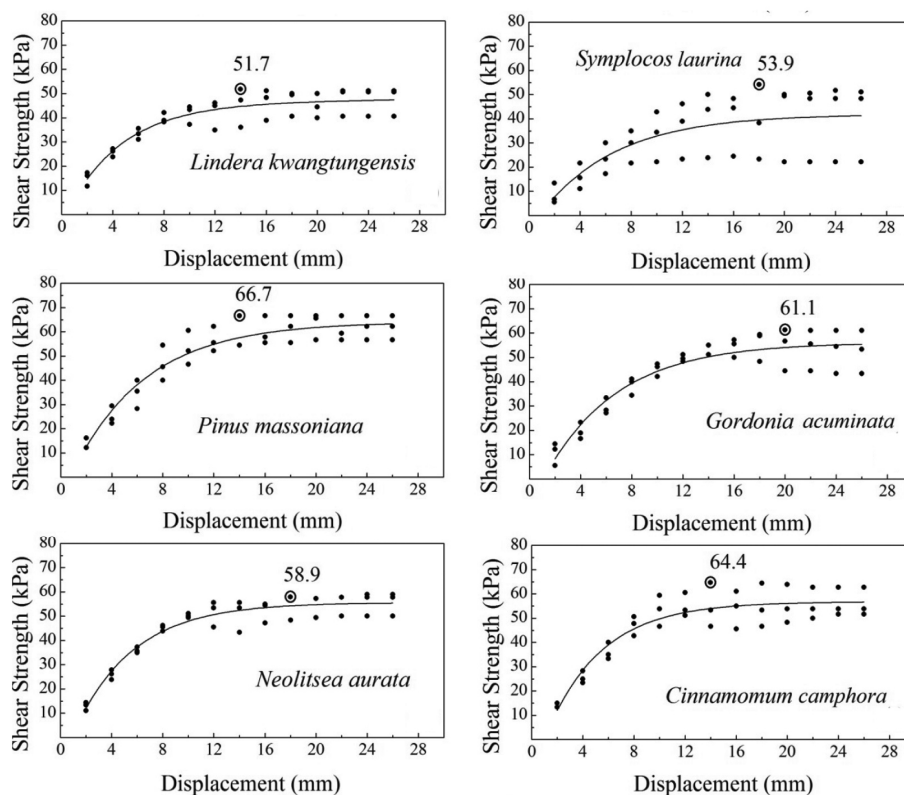


Figure 5. Correlation of shear strength and shear displacement of tree species roots. Each species had three repeats.

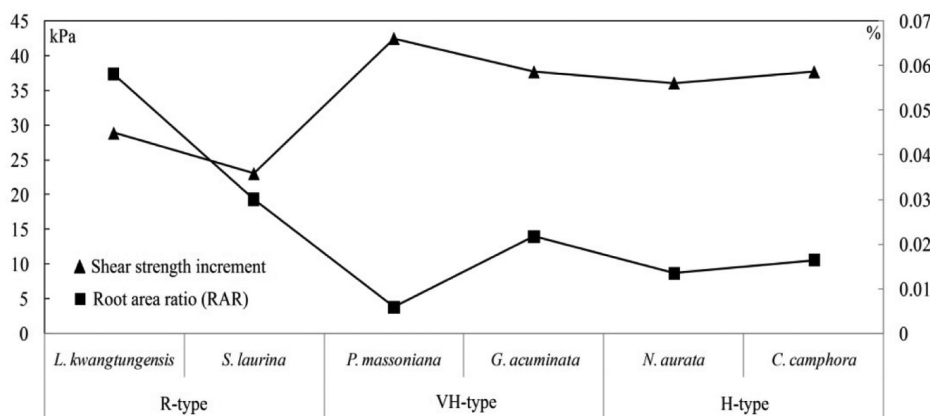


Figure 6. Relationship of shear strength increment and RAR for different tree species.

from the intersection point of the roots and shear plane. Inclined line represents the actual distribution of roots on shear direction and vertical line represents the distance of the roots to the centre of shear plane. Figure 7 shows that the five red lines (0.2, 0.4, 0.8, 1.2 and 1.6 mm of width, respectively) correspond to the root diameter of 0–2, 2–4, 4–6, 6–8 and >8 mm respectively. Except *G. acuminata*, other plant roots were all distributed in the range 0–60°. VH-type and R-type roots were distributed at 30–60°, H-type was distributed at 0–60°. There was a maximum root quantity at 0–30° of *L. kwangtungensis*. In addition,

tapered root (VH-type) was distributed at 0–10 cm and there was no result in other two root architectures. *L. kwangtungensis* had the smallest root distribution area but had the most number of roots with diameter greater than 4 mm. *N. aurata* had the widest range of root distribution against the shear direction (15 cm). There were more fine roots (diameter <2 mm) in *P. massoniana* and *C. camphora*. Similarly, thicker roots (diameter >2 mm) were found in *G. acuminata* and *N. aurata*. For R-type of *S. laurina* and *L. kwangtungensis*, presence of thin and thick roots was not obvious.

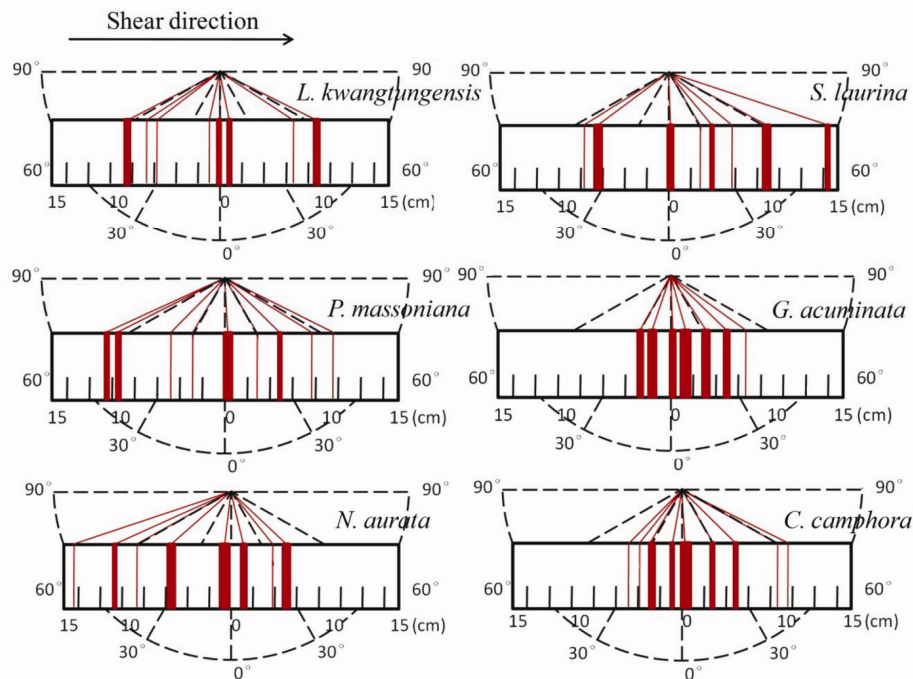


Figure 7. Inclination and distribution properties of roots for different tree species. Boundary of root distribution is 15 cm (Scale unit in cm).

Stress propagation simulation

Simulations of stress propagation under point load (Figure 8 a) represent the condition of soil samples without roots; Figure 8 b–d represents condition of soil samples with fine roots with a distance to the breakdown point at 50, 100 and 150 mm respectively. Figure 8 e–g shows conditions similar to those of Figure 8 b–d but with thick roots in rooted soil samples. Figure 8 h–j shows soil samples with oblique fine roots, which have an angle with shear plane of 34°, 45° and 64° respectively. Stress simulations are considered only in the horizontal direction. Smaller negative value of stress indicates that there was a higher force applied on soil samples. Darker areas existed behind roots in soil samples and represent the contributions of roots on resistance of stress propagation. Simulation results showed that intensive stress area existed near the point load in all situations. Elastic deformation appeared in all soil samples despite the existence of roots. There were low stress distribution areas on the upper and lower sides of point load. Stress propagations spread from the point load to the other side circularity (Figure 8). In case of Figure 8 b–d, roots which were closer to the point load had shorter stress propagation distance, and the distribution of stress was more uniform. Lower stress area showed up closer to point load when roots were located near the point load. Shear failure could not happen when loose stress distribution area was far from the boundary. Comparison of Figure 8 b–d with e–g shows that thick roots could withstand more stress than fine roots in rooted soil samples. A smaller extreme stress

existed in each unit behind the roots (in the cases of c, d and f, g). Stress propagations during shearing of two groups (b, c, d and e, f, g) were remarkably similar despite thickness of the roots. In other words, stress distribution showed no relationship with root diameter. When an oblique root existed in soil samples, stress propagation changed with the angle of roots inclination. When roots had an angle of 34° with shear plane, these contributions on resistance of stress propagation were good.

Discussion

Variations of soil shear strength increment for different tree species

Different species have different effects on soil shear strength reinforcement (Figure 5, Table 4). Results showed that for tall tree species such as *P. massoniana* and *C. camphora*, rooted soil samples were easily destroyed due to low shear peak strength displacement (12 mm) during shear failure. For small tree species such as *G. acuminata*, *N. aurata* and *S. laurina*, they often provided a longer shearing process. However, shear strength of tall tree species was much higher than small tree species after shear failure occurred. During the process of plant growth, contents of cellulose and lignin in roots slowly change. When the root is young, cellulose content will be more than lignin. However, when the root matures, an opposite relationship exists in the root component²⁴. Higher cellulose content in small tree species roots meant that bending capacity was greater but shear

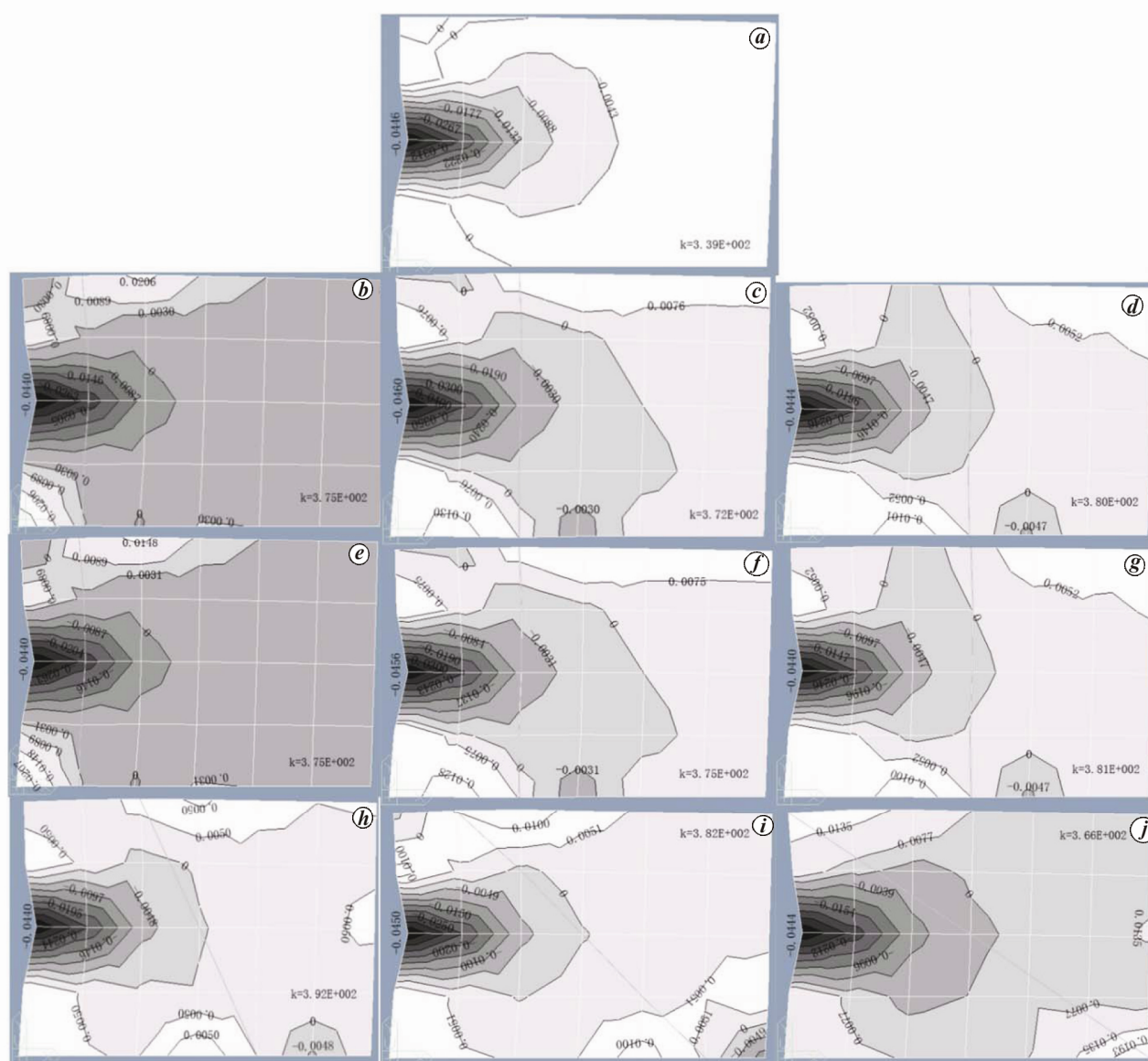


Figure 8. Simulation of stress propagation under different conditions. Darker colours represented greater stress. Negative value of soil samples represented is compressed. Positive value of soil samples represented is stretched.

strength was lower than tall tree species, which was also reported by Genet *et al.*²⁵. Burylo and Hudek²⁶ studied different forest categories and their soil shear strength enhancements and found that roots of shrubs (also regarded as mature roots) had the highest effect on soil shear strength increment, followed by herbs and young trees. Mature roots could provide better shear strength reinforcement than young tree roots. In the case of *L. kwangtungensis*, root reinforcement was lower than that observed for the three small tree species. High lignin content might be the cause of this phenomenon and this requires further research.

Results of ΔS_w and ΔS_t (Table 4) showed that the theoretical values were much higher than the experimental

values (values obtained by shear test). Although Wu's model had proved overestimated soil shear strength⁹, ΔS_t was 2–20 times lesser than ΔS_w . Relationship of ΔS_w with tree species was contrary to ΔS_t . R-type was deemed to have the best behaviour of resistance using Wu's method, followed by H-type and VH-type tree species roots. Root quantity and RAR had contributed more on shear increment⁹. Frictions in soil–root interface and root architecture were two main factors for the behaviour of shear strength. However, in this study, soil–root interfacial friction was not contained in shear test, which meant ΔS_t was only affected by root architecture and root properties. When the influence of root architecture on soil shear strength increment was considered, tapered root

Table 4. Values of six tree species root on soil shear strength reinforcement

Species	<i>L. kwangtungensis</i>	<i>S. laurina</i>	<i>P. massoniana</i>	<i>G. acuminata</i>	<i>N. aurata</i>	<i>C. camphora</i>
ΔS_w (kPa)	438.6	473.7	61.3	211.9	222.2	272.3
ΔS_t (kPa)	28.8	23.0	42.4	27.4	36.0	37.6
Efficiency (%)	6.6	4.9	69.2	17.7	16.2	13.8

(VH-type, 42.4 kPa and 27.4 kPa) showed highest enhancement. In order to compare the contribution of root architecture on shear increment, we introduced a concept called ‘efficiency of root architecture’. For VH-type and H-type roots (except for *P. massoniana*), efficiency of root architecture was around 10–20%. For R-type root, this was 5–10%. In general, taproots and widely distributed roots had performed much better than oblique roots. As the one with lowest RAR value and root quantity, difference between ΔS_w and ΔS_t of *P. massoniana* was not obvious.

Analysis of root properties and branching characteristics on soil shear strength

It was concluded that root diameter class, RAR and root tensile strength had no obvious relationship with shear strength increment (Tables 2 and 3 and Figure 6). Due to various growth forms and environmental heterogeneity, root diameter class was different among many species²⁷. Based on our results, root diameter class and RAR could not be used to reflect effects of roots on soil reinforcement while considering only the influence of root architecture. For root tensile strength, b value was significantly higher than that in other studies (ranged from -0.52 to -0.11 , but in this study, ranged from -1.06 to -0.48)^{23,25}. During simulation of stress propagation (Figure 8), influence of root thickness had no obvious relationship with stress propagation line. However, resistance was increased with thickness of roots. When shear failure occurred, thick roots could provide a greater resistance than thin roots. If thick roots are connected to each other, a more stable structure would appear in resistance to shear failure²⁸.

During shear failure, due to unequal shear forces in shear plane¹⁴, roots that were destroyed first, experienced much greater shear forces than roots at the back in the rooted soil samples. *C. camphora* and *N. aurata* (H-type) had the most wide distribution of roots, which provided a stronger soil shear strength enhancement (the second good performance of root reinforcement). When roots were widely distributed in soil, their contributions to soil reinforcement became much stronger than roots gathered near taproots (Figure 8 *b–g*). Roots located in top soil were usually formed with reticular formation in the field. When shear forces are applied on this section, in addition to their own tensile stress, roots in reticular formation play an important role of resisting shear failure. Inclination of roots also had an effect on soil shear strength

increment. Stress distribution in rooted soil samples showed a linear relationship with root angle (only at the range of 35° – 65°) (Figure 7 and Figure 8 *h–j*). In Figure 8 *h*, two loose stress areas existed symmetrically in the centre of the oblique root. Then these two loose stress areas moved to the corner of rooted soil samples with a decrease in root angle as shown in Figure 8 *i, j*. In other words, the capacity of roots on resistance of shear failure became stronger with decreasing root inclination (only at the range of 35° – 65°), which was in agreement with Fan and Chen’s study⁹. However, this could not be observed in our shear tests.

In case of root architecture, results showed that tapered roots (VH-type, 42.4 kPa and 27.4 kPa) showed maximum soil reinforcement; followed by widely distributed root architecture (H-type, 37.6 kPa and 36.0 kPa) and then oblique root (R-type, 28.8 kPa and 23.0). These results differed with Fan and Chen’s study⁹ who showed that R-type had the best behaviour of increment with the most number of inclined roots which showed a greater shear capacity. However, their experiments were based on *in situ* rooted soil samples, which were different from ours. In our study, root structure was collected from the field and reloaded in shear box in the lab. The original friction between roots and soil (friction under natural condition) had been destroyed and no function on resistances to shear failure. In other words, friction between roots and soil might contribute more than the effect of root architecture of *in situ* rooted soil for R-type. When only root architecture was considered, R-type seemed to have a bad resistance to shear failure. In addition to root inclination, deep and thick taproots and widely distributed roots played significant roles on soil shear strength increment. They resisted the deformation of rooted soil samples. After the soil deformed, rooted soil samples still had residual shear strength, which were mostly caused by roots^{29–31}. However, influence of root architecture on resistance to further shearing was not studied in this study. Since different root characteristics (i.e. root number and diameter) or environmental factors (i.e. soil and climate)³² resulted in different root architectures, detailed investigations are needed to be carried out especially for a certain study area.

Conclusion

Based on the experiments of direct shear tests on six tree species roots and the analysis of root diameter class,

RAR, root tensile strength, inclination and distribution, the effects of roots on soil shear strength increment were studied and discussed. Root architecture that contained taproots (VH-type) and widely distributed roots (H-type) showed larger shear strength increment than root architecture that contained oblique roots (R-type), when the initial friction between soil and root was ignored. When thick, widely distributed roots exist in the root system, resistance of root architecture to shear failure would be stronger. Root properties of root diameter class and RAR had no relationship with shear strength increment, which meant that they cannot be used to reflect the effects of root architecture on soil shear strength increment. To estimate different tree species roots on soil shear strength increment in the field, initial friction between soil and roots should be considered as important as root architecture.

Conflict of interest: The authors declare no conflict of interest.

1. Gray, D. H. and Robbin, B. S., *Biotechnical and Soil Bioengineering Slope Stabilization: A Practical Guide for Erosion Control*, John Wiley, 1996.
2. Waldron, L. J., The shear resistance of root-permeated homogeneous and stratified soil. *Soil Sci. Soc. Am. J.*, 1977, **41**(5), 843–849.
3. Ziemer, R. R., *Roots and the stability of forested slopes. Erosion and Sediment Transport in Pacific Rim Steeplands*, IAHS Publ. no. 132, Christchurch, New Zealand, 1981, pp. 343–361.
4. Nilaweera, N. S. and Nutalaya, P., Role of tree roots in slope stabilization. *B. Eng. Geol. Environ.*, 1999, **57**, 337–342.
5. Greenway, D. R., *Vegetation and Slope Stability*, John Wiley & Sons, 1987.
6. Gyssels, G., Poesen, J., Bochet, E. and Li, Y., Impact of plant roots on the resistance of soils to erosion by water: a review. *Prog. Phys. Geog.*, 2005, **29**(2), 189–217.
7. Stokes, A., Atger, C., Bengough, A. G., Fourcaud, T. and Sidle, R. C., Desirable plant root traits for protecting natural and engineered slopes against landslides. *Plant Soil*, 2009, **324**(1–2), 1–30.
8. Cohen, D., Schwarz, M. and Or, D., An analytical fiber bundle model for pullout mechanics of root bundles. *J. Geophys. Res.*, 2011, **116**, F03010; doi:10.1029/2010JF001886.
9. Fan, C. C. and Chen, Y. W., The effect of root architecture on the shearing resistance of root-permeated soils. *Ecol. Eng.*, 2010, **36**(6), 813–826.
10. Reubens, B., Poesen, J., Danjon, F., Geudens, G. and Muys, B., The role of fine and coarse roots in shallow slope stability and soil erosion control with a focus on root system architecture: a review. *Trees*, 2007, **21**(4), 385–402.
11. Wu, T. H., McKinnell III, W. P. and Swanston, D. N., Strength of tree roots and landslides on Prince of Wales Island, Alaska. *Can. Geotech. J.*, 1979, **16**(1), 19–33.
12. Docker, B. B. and Hubble, T. C. T., Quantifying root-reinforcement of river bank soils by four Australian tree species. *Geomorphology*, 2008, **100**(3), 401–418.
13. Fan, C. C. and Su, C. F., Role of roots in the shear strength of root-reinforced soils with high moisture content. *Ecol. Eng.*, 2008, **33**(2), 157–166.
14. Pollen, N. and Simon, A., Estimating the mechanical effects of riparian vegetation on streambank stability using a fiber bundle model. *Water Resour. Res.*, 2005, **41**, 1–11.
15. Mickovski, S. B., Stokes, A., Van Beek, R., Ghestem, M. and Fourcaud, T., Simulation of direct shear tests on rooted and non-rooted soil using finite element analysis. *Ecol. Eng.*, 2011, **37**(10), 1523–1532.
16. Greenwood, J. R., SLIP4EX – a program for routine slope stability analysis to include the effects of vegetation, reinforcement and hydrological changes. *Geotech. Geol. Eng.*, 2006, **24**, 449–465.
17. Giadrossich, F., Schwarz, M., Cohen, D., Preti, F. and Or, D., Mechanical interactions between neighboring roots during pullout tests. *Plant Soil*, 2013, **367**(1–2), 391–406.
18. Yen, C. P., Tree root patterns and erosion control. In *Proceedings of the International Workshop on Soil Erosion and its Countermeasures* (ed. Jantawat, S.), Soil and Water Conservation Society of Thailand, Bangkok, 1987.
19. Prasad, A., Kazemian, S., Kalantari, B., Huat, B. B. and Mafian, S., Stability of tropical residual soil slope reinforced by live pole: experimental and numerical investigations. *Arab. J. Sci. Eng.*, 2012, **37**(3), 601–618.
20. FAO, I., World reference base for soil resources. *World Soil Resour. Rep.*, 1998, **84**, 21–22.
21. Operstein, V. and Frydman, S., The influence of vegetation on soil strength. *Proc. Inst. Civ. Eng. Ground Improv.*, 2000, **4**(2), 81–89.
22. Fan, C. C. and Lai, Y. F., Influence of the spatial layout of vegetation on the stability of slopes. *Plant Soil*, 2014, **377**(1–2), 83–95.
23. Bischetti, G. B., Chiaradia, E. A., Simonato, T., Speziali, B., Vitali, B., Vullo, P. and Zocco, A., Root strength and root area ratio of forest species in Lombardy (Northern Italy). *Plant Soil*, 2005, **278**(1–2), 11–22.
24. Ghestem, M., Sidle, R. C. and Stokes, A., The influence of plant root systems on subsurface flow: implications for slope stability. *BioScience*, 2011, **61**(11), 869–879.
25. Genet, M., Stokes, A., Salin, F., Mickovski, S. B., Fourcaud, T., Dumail, J. F. and van Beek, R., The influence of cellulose content on tensile strength in tree roots. *Plant Soil*, 2005, **278**(1–2), 1–9.
26. Burylo, M., Hudek, C. and Rey, F., Soil reinforcement by the roots of six dominant species on eroded mountainous marly slopes (Southern Alps, France). *Catena*, 2011, **84**(1), 70–78.
27. Craine, J., Competition for nutrients and optimal root allocation. *Plant Soil*, 2006, **285**, 171–185.
28. Zobel, R. W., Primary and secondary root systems. Root and soil management: interaction between roots and the soil. *Agronomy Monograph*, 2005, **48**, 3–14.
29. Yan, Z. X., Yan, C. M. and Wang, H. Y., Mechanical interaction between roots and soil mass in slope vegetation. *Sci. China Technol. Sci.*, 2010, **53**(11), 3039–3044.
30. Yan, Z. X., Song, Y., Jiang, P. and Wang, H. Y., Mechanical analysis of interaction between plant roots and rock and soil mass in slope vegetation. *Appl. Math. Mech.*, 2010, **31**, 617–622.
31. Schwarz, M., Cohen, D. and Or, D., Spatial characterization of root reinforcement at stand scale: theory and case study. *Geomorphology*, 2012, **171**, 190–200.
32. Hodge, A., The plastic plant: root responses to heterogeneous supplies of nutrients. *New Phytol.*, 2004, **162**, 9–24.

ACKNOWLEDGEMENTS. The research is supported by the Fundamental Research Funds for the Central Universities (No. 2016ZCQ06 and No. 2015ZCQ-SB-01) and the experimental study on water conservation materials for afforestation in Zhangjiakou, Hebei province (2014HXFWSBXY003).

Received 23 April 2017; revised accepted 14 November 2017.

doi: 10.18520/cs/v114/i06/1250-1260